JOURNAL OF GEOPHYSICAL RESEARCH, VOL. 112, D01204, doi:10.1029/2005JD006828, 2007

Direct radiative effect modeled for regional aerosols in central Europe including the effect of relative humidity

G. Iorga,[1,2] R. Hitzenberger,[3] A. Kasper-Giebl,[1] and Hans Puxbaum[1]

Received 27 October 2005; revised 17 July 2006; accepted 28 July 2006; published 13 January 2007.

[1] In view of both the climatic relevance of aerosols and the fact that aerosol burdens in central Europe are heavily impacted by anthropogenic sources, this study is focused on estimating the regional-scale direct radiative effect of aerosols in Austria. The aerosol data (over 80 samples in total) were collected during measurement campaigns at five sampling sites: the urban areas of Vienna, Linz, and Graz and on Mt. Rax (1644 m, regional background aerosol) and Mt. Sonnblick (3106 m, background aerosol). Aerosol mass size distributions were obtained with eight-stage (size range: 0.06–16 μm diameter) and six-stage (size range 0.1–10 μm) low-pressure cascade impactors. The size-segregated samples were analyzed for total carbon (TC), black carbon (BC), and inorganic ions. The aerosol at these five locations is compared in terms of size distributions, optical properties, and direct forcing. Mie calculations are performed for the dry aerosol at 60 wavelengths in the range 0.3–40 μm. Using mass growth factors determined earlier, the optical properties are also estimated for higher relative humidities (60%, 70%, 80%, and 90%). A box model was used to estimate direct radiative forcing (DRF). The presence of absorbing species (BC) was found to reduce the cooling effect of the aerosols. The water-soluble substances dominate radiative forcing at the urban sites, while on Rax and Sonnblick BC plays the most important role. This result can be explained by the effect of the surface albedo, which is much lower in the urban regions (0.16) than at the ice and snow-covered mountain sites. Shortwave (below 4 μm) and longwave surface albedo values for ice were 0.35 and 0.5, while for snow surface albedo, values of 0.8 (shortwave) and 0.5 (longwave) were used. In the case of dry aerosol, especially for urban sites, the unidentified material may contribute a large part to the forcing. Depending on the sampling site the estimated forcing gets more negative with increasing humidity. When humidity changes from 50% to 90%, the factor of forcing change for Graz is about 3 times larger than that for Linz (3.8) and about 5 times greater than that for Vienna (2.4). At the mountain stations the change in forcing with increasing humidity is much less pronounced because of the high surface albedo. The influence of the aerosol mixing state on the single-scattering albedo as well as on DRF is investigated for all sampling sites. As expected, the single-scattering albedo was found to have lower values for internal mixture than for external mixture.

Citation: Iorga, G., R. Hitzenberger, A. Kasper-Giebl, and H. Puxbaum (2007), Direct radiative effect modeled for regional aerosols in central Europe including the effect of relative humidity, *J. Geophys. Res.*, *112*, D01204, doi:10.1029/2005JD006828.

1. Introduction

[2] The effect of tropospheric aerosols on global climate is usually discussed in terms of the direct and the indirect effect, and most recently, the semidirect effect. In the direct effect, light scattering by aerosol particles results in a negative radiative forcing (cooling effect), as part of the solar flux is scattered back to space. If the particles contain absorbing material, total forcing can become positive (heating effect), as the energy absorbed by the particles leads to an increase of thermal radiation [e.g., *Haywood and Shine*, 1995]. Aerosol particles acting as cloud condensation nuclei can change the radiative properties of a cloud as well as the cloud's lifetime (indirect effect, [*Twomey*, 1977; *Albrecht*, 1989; *Pincus and Baker*, 1994]). If absorbing particles are present in elevated layers, radiative heating in these layers can perturb the temperature profile, which can lead to evaporation of low-level clouds (semidirect effect [*Hansen et al.*, 1997; *Ackerman et al.*, 2000]).

[3] In order to be able to formulate reliable policy recommendations in the context of climate protection, a

[1]Institute for Chemical Technology and Analytics, Vienna University of Technology, Vienna, Austria.
[2]Now at Department of Physics, Faculty of Chemistry, University of Bucharest, Bucharest, Romania.
[3]Faculty of Physics, Institute for Experimental Physics, University of Vienna, Vienna, Austria.

0148-0227/07/2005JD006828$09.00

quantitative understanding of the role of absorbing and nonabsorbing aerosols is required. The *IPCC* [2001] report shows estimates of the global and annual mean direct radiative forcing for the period from preindustrial (1750) to present day (2000) due to sulfate (-0.4 W/m^2), biomass burning (-0.1 W/m^2), fossil fuel OC (-0.1 W/m^2) and fossil fuel BC (+0.2 W/m^2) as well as the uncertainties of these values. The distribution of radiative forcing calculated by the global models necessarily has a limited spatial resolution with typical grid sizes between 1 and 5 degrees in latitude or longitude. In a study of an external mixture of black carbon (BC), organic carbon (OC) and sulfate, *Penner et al.* [1998] reported that aerosols originating from biomass burning act to cool the earth/atmosphere system causing a radiative forcing between -0.16 and -0.23 W/m^2, while BC and associated OC from fossil fuel combustion could heat the system through a radiative forcing between +0.16 and +0.20 W/m^2. Annual average negative forcing by aerosols ranges from -0.53 to -0.81 W/m^2 and dominates the positive forcing by BC from fossil fuels, particularly in the Northern Hemisphere summer. On the other hand, an internal mixture of BC and sulfate would increase the amount of absorbed radiation, and could decrease the overall net forcing by 20 to 60% [*Haywood and Shine*, 1995]. Comparisons of forcing predictions with sun photometer measurements [*Sato et al.*, 2003] show that forcing by total BC aerosols (i.e., including BC from biomass burning) are rather of the order of +0.5 W/m^2. *Chung and Seinfeld* [2002] give the forcing by BC as +0.51 and +0.8 W/m^2 (for externally and internally mixed BC). All global studies of the radiative effects of BC aerosols use BC concentrations obtained from emission inventories [e.g., *Bond et al.*, 2004; *Cooke and Wilson*, 1996]. It should be noted, however, that these concentrations often do not agree with measured data that are consistently larger by factors of about 2 [e.g., *Schaap et al.*, 2004] or 3–4 [*Chung and Seinfeld*, 2002].

[4] Apart from the geographical resolution and uncertainties of emission inventories, major uncertainties in the estimates of radiative forcing by aerosols are caused by insufficient knowledge of the physical (size, shape, size distribution and refractive index) and chemical characteristics of tropospheric aerosols. Consequently, an improvement of the estimates of the aerosol direct forcing requires extensive observations, including physical (such as number or mass size distributions) and chemical (such as composition) measurements of the aerosol that can be obtained from field campaigns in selected regions. Although information on the chemical composition of bulk aerosol samples has improved over the last decade (for European aerosols, see e.g. the overview given by *Putaud et al.* [2004]), measurement data on BC, its size distribution and mixing state are still rather scarce.

[5] The aim of this research was to estimate the direct radiative forcing caused by central European aerosols and to investigate its variability with relative humidity and ground cover (urban surface, ice, snow). The aerosol data we have cover both urban and background regions as well as winter and summer seasons with an additional campaign in spring in Vienna. Instead of synthetic aerosol data obtained from emission inventories, we used measured data collected at five sampling sites in Austria (one large and two midsize urban areas as well as two mountain stations; all located within one grid point of a global aerosol model). The relevant optical parameters extinction, scattering and absorption coefficients as well as the optical depth and the single-scattering albedo in the wavelength range from 0.3 to 40 μm were calculated from measured mass size distributions of inorganic ions, minerals and BC. These parameters were used as input for a box model to estimate the direct radiative effect of the dry aerosol under cloud-free conditions. The effect of relative humidity on the total forcing by the aerosol was investigated using measured aerosol mass growth factors obtained earlier [*Hitzenberger et al.*, 1997]. The only input parameters that were not measured were the wavelength dependent refractive indices of the different chemical fractions. These data were taken from the model by *D'Almeida et al.* [1989], which is the basis for the widely used OPAC model [*Hess et al.*, 1998].

2. Experimental Methods and Data Preparation

[6] The aerosol data had been collected previously in different studies. The most recent data (collected in 2001 in Linz and Graz) belong to the AUPHEP study of the Austrian Academy of Sciences [*Hauck et al.*, 2004], while the earlier measurement campaign in Vienna as well as the Sonnblick and Rax campaigns were performed within studies funded by the Austrian Science Fund. Because of the different aims of the studies as well as the different aerosol conditions at the sites, sampling schedules varied from campaign to campaign. In this study, we use only those data sets where we have a comprehensive set of size selective chemical analyses. In total, we have 82 data sets (19 for Vienna, 24 and 25 for Linz and Graz, and 7 each for Rax and Sonnblick).

2.1. Sampling Sites and Methods

[7] Ambient aerosol samples were taken using two kinds of Berner-type low-pressure cascade impactors. Table 1 shows an overview of the sampling sites and measurement periods, while Tables 2a and 2b give the characteristics of the impactors (cut sizes are given in terms of aerodynamic equivalent diameter). In Vienna, all sampling times were 12 hours. In Linz and Graz, sampling times in winter were 12 hours, while summer sampling times were 24 hours. At Sonnblick and Rax the sampling times were chosen depending on the weather situation to collect adequate sample masses. At both mountain stations, sampling was performed only under no-cloud conditions.

[8] The impactors were loaded with suitable sampling substrates. Aluminium foils preheated for one hour at 500°C were used for total carbon (TC) and elemental carbon (EC) analysis. BC was analyzed from cellulose diacetate substrates. Chemical analyses were mostly performed either from the aluminium foils (Vienna, Sonnblick) or from precleaned Tedlar foils.

[9] At the Vienna site, samples were collected at the roof laboratory of the Institute for Experimental Physics in central Vienna (population 1.8 million) at circa 35 m above ground. The aerosol at that height is rather well mixed and not impacted directly by sources [*Hitzenberger and Puxbaum*, 1993]. Sampling was performed outside the heating season, but even then, direct impacts from nearby

Table 1. Overview of Sampling Sites

Site	Site Code	Coordinates/Altitude	Measurement Period	Resolution	Number of Samples
Vienna (urban, large)	V	48°13′N 16°21′E/203 m above mean sea level	29 April 1996 to 12 May 1996	12 hours	19
Linz (urban, midsize)	L	48°19′N 14°17′E/266 m above mean sea level	15 January 2001 to 23 January 2001 and 08 August 2001 to 14 August 2001	12 hours/23 hours	24
Graz (urban, midsize)	G	47°04′N 15°30′E/545 m above mean sea level	15 January 2001 to 23 January 2001 and 08 August 2001 to 14 August 2001	12 hours/23 hours	25
Mt. Rax (regional background)	R	47°53′N 15°59′E/1644 m above mean sea level	07 March 2000 to 24 March 2000	variable	7
Mt. Sonnblick (background)	S	47°03′N 12°58′E/3106 m above mean sea level	23 May 1993 to 05 June 1993	variable	7

chimneys (with effective stack heights above the height of our sampling site) are not expected to have much influence as most of the heating energy in Vienna is (data for 2003, *Hitzenberger et al.* [2006]) provided by natural gas (32.2%) and district heating plants (43.5%). The Vienna samples were analyzed for inorganic ions, minerals, TC and BC.

[10] At both Linz and Graz sites the measurements were performed during the project AUPHEP. Linz (population 203000) is located N of the Alps on the Danube. It has one of Austria's largest heavy industry conglomerates and is therefore predominantly affected by industrial emissions (iron and steel plants, chemical industry), which can cause rather high pollutant concentrations during stagnant conditions. The sampling site was situated within a large residential area. Graz (population 240,000) is situated S of the Alps in a semialpine basin. There is no heavy industry, but the weak natural ventilation in this basin often causes high pollution levels, especially in wintertime when long lasting inversion situations are typical. The sampling site was located in a mixed residential/commercial area and near a road with medium traffic load. The AUPHEP samples were analyzed for inorganic ions, minerals, TC and EC.

[11] At Mt. Rax a 4-week campaign was carried out in March 2000. Mt. Rax is situated circa 100 km SSW of Vienna. The sampling site was at an alpine shelter (Otto-haus) at the eastern rim of the Rax plateau at 1644 m above mean sea level. During the campaign, only the field team stayed at the shelter, which was closed to the public all winter. Electricity was used for cooking and heating in order to keep local pollution at a minimum. The prevailing wind direction was from the West, where the nearest upwind anthropogenic sources (small villages in mountain valleys) are more than 100 km distant. (Details of the site can be found elsewhere; see *Hitzenberger et al.*, 2001]. Wintry conditions with frequent snowfalls and temperatures below 0°C prevailed, so the ground (alpine meadows and dwarf pines) was covered with fresh snow. The Rax samples were analyzed for inorganic ions, minerals, TC, BC and EC.

[12] Mt. Sonnblick (3106 m above mean sea level) is a mountain peak located in the central range of the Austrian Alps. Measurements there were performed during a 2-week intensive campaign (May/June 1993) at the Sonnblick Observatorium, which is located on a rocky outcrop above a glacier. Because of its height, this site receives free troposphere air most of the time, but under daytime no-cloud conditions in summertime, boundary layer air masses are transported upwards by the valley wind systems [e.g., *Seibert et al.*, 1998]. Details on the site and sampling procedures are described elsewhere [*Hitzenberger et al.*, 2000]. The Sonnblick samples were analyzed only for inorganic ions, minerals, and TC. BC (or EC) was not measured, so the contribution of BC had to be estimated. As both Rax and Sonnblick are background sites, the BC/TC ratio as well as the size distribution of BC should be rather similar, so we used the average BC size distribution measured for the Rax aerosol as representative for the Sonnblick BC size distribution and estimated the total BC mass for the Sonnblick samples from the measured TC mass (with BC/TC = 0.478 at Rax). This value is also in the range found at other background sites influenced by anthropogenic pollution. In the INDOEX experiment, e.g., BC/TC values were between 0.5 and 0.7 over the Indian Ocean when air masses came from the Indian Subcontinent [*Quinn et al.*, 2002]. During the NEAQS study off the New England coast, however, EC/TC ratios were much lower (circa 0.09; [*Bates et al.*, 2005]; particulate organic matter even dominated over sulfate under some flow conditions). The BC/TC values measured at Rax are very similar to BC/TC values for fossil fuel combustion (0.5, [*Novakov et al.*, 2000]).

2.2. Chemical Analysis

[13] The size-segregated samples were analyzed for total gravimetric mass on a Mettler ME3 microbalance (accuracy

Table 2a. Impactor Types Used at the Sites for Collecting Samples for Chemical Analyses[a]

Site	Impactor
Vienna	Six-stage
Linz	Eight-stage for PM Six-stage for EC and ions
Graz	Eight-stage for PM Six-stage for EC and ions
Mt. Rax	Six-stage
Mt. Sonnblick	Six-stage

[a]If only one impactor type is given for a site, parallel sampling with up to three identical impactors was performed.

Table 2b. Nominal Lower Cut Sizes of the Stages of the Two Impactor Types[a]

	Lower Cut Diameter d_{ae}, μm	
Stage	Six-Stage	Eight-Stage
1	0.1	0.06
2	0.212	0.13
3	0.464	0.26
4	1.0	0.51
5	2.12	1.0
6	4.64	2.0
7[b]	10.0	-
7		4.0
8		8.0
9[b]		16.0

[a]All sizes are given as aerodynamic equivalent diameters.
[b]Stages 7 and 9 (of the six-stage and eight-stage impactors, respectively) are only used as preprecipitators of large particles. Deposits on these stages are not analyzed.

±3 μg). Total carbon (TC) was determined using a combustion method [*Puxbaum and Rendl*, 1983]. For black carbon (BC) an optical method (integrating sphere method originally developed by *Heintzenberg* [1982]; description of current method is by *Hitzenberger and Tohno* [2001]) was used. Soluble ions (NH_4^+, Na^+, K^+, Ca^{2+}, Mg^{2+}, SO_4^{2-}, NO_3^- and Cl^-) were analyzed by ion chromatography.

[14] For the ion determination, an aliquot of each impactor foil was extracted with ultra pure water in an ultrasonic bath. Analysis was performed with standard procedures (anions: Dionex AS12A, electrochemical suppression SRAS, sodium carbonate/bicarbonate eluent, eluent flow 1,5 mL/min; cations: Dionex CS12A, electrochemical detection CSRS, methansulfonic acid eluent, eluent flow 1 mL/min). Detection limits for the ions were in the range of 5–30 μg/mL extract, which translates to 10–600 ng/m^3 for 12 hour samples and half as much for the 24 hour samples. Ca^{2+} and Mg^{2+} were assumed to be present as carbonates, even though we have no information on insoluble Ca and Mg. The concentrations of these ions were multiplied by 3.47 and 3.5 respectively to account for the CO_3^- mass.

[15] TC was determined with a combustion method based on the setup described by *Puxbaum and Rendl* [1983]. An aliquot of each impactor foil was combusted in an oven at 1000°C in an oxygen stream. The evolving CO_2 was determined with a NDIR analyzer (Maihak UNOR 6B). EC was determined from another aliquot of the substrate by a two-step combustion method using the operational parameters (2 hour treatment at 340°C in O_2 atmosphere) described by *Cachier et al.* [1989]. Afterwards the pretreated filters are combusted at 1000°C, just as for TC analysis. The absolute detection limit of the method is 0.2 μg TC, determined from 3σ of standards with low concentration.

[16] For the BC analysis, the loaded sampling substrates were put into PE vessels, rinsed with 5 mL of a mixture of ultrapure water and isopropanol (80:20) and then dissolved in 20 mL acetone. The resulting liquid suspensions were put into the integrating sphere. The signal loss (at 550 nm) caused by the presence of light absorbing material was attributed to BC using a calibration curve obtained with a commercial carbon black (Elftex 125, Cabot Corp.). Details of the analysis method can be found in the study by *Hitzenberger and Tohno* [2001]. The detection limit is 2 μg BC, which translates to 40 ng/m^3 for typical impactor sampling times.

2.3. Calculation of Optical Parameters

[17] The optical parameters necessary as input for the forcing calculations (see below) were calculated using the Mie routine BHMIE [*Bohren and Huffman*, 1983]. The absorption coefficient $\sigma_{abs}(\lambda)$ of spherical particles at wavelength λ, e. g., is obtained from the absorption efficiency factor $Q_{abs}(\lambda, d, m)$ using

$$\sigma_{abs}(\lambda) = \int \frac{\pi d^2}{4} Q_{abs}(\lambda, d, m) n(d) dd \quad (1)$$

where d denotes the particle's diameter (spherical particles), m the complex refractive index and n(d) the number size distribution of the aerosol. The scattering coefficient σ_{sc} is obtained in the same way using the scattering efficiency factor $Q_{sc}(\lambda,d,m)$. Calculations were performed for 60 wavelengths in the range from 0.3 to 40 μm. Wavelength-dependent refractive indices were taken from the MIM model [*D'Almeida et al.*, 1989], which are the same as for the OPAC code [*Hess et al.*, 1998].

[18] Lognormal functions for the mass size distributions were obtained from the size segregated impactor samples using an iterative procedure [*Lürzer*, 1980]. A lognormal distribution function was fitted first to the data in the submicron range, where a distinct mass mode was always present. Subtracting the calculated contribution of this mode from the mass deposits on the stages in the coarse size range yielded the basis for fitting a lognormal function also for the coarse mode. The contribution of this coarse mode to the aerosol in the fine particle range was calculated and subtracted from the mass deposits on the relevant stages. Another lognormal function was fitted through the remaining mass deposits, etc. The procedure usually converges after three iterations and the characteristic parameters (mass median diameter, geometric standard deviation and total modal mass) of the fine and coarse modes do not change by more than a few percent in further iterations. At the end of the fitting procedure, the fitted size distributions are checked against the measured data for consistency and mass conservation. The parameters of the nucleation mode could not be obtained from the impactor measurements, because the size range below 0.1 μm was either beyond the lower cut size of the impactor or the impactors had too little size resolution in this range.

[19] In some cases, only one distinct mode (the one in the fine particle size range) was found for the samples collected with the six-stage impactors, so only this mode was used in the calculations. As the coarse aerosol contributes only little to the total scattering and absorption coefficients of the aerosol, neglecting the coarse particles gives only slight underestimations of the optical parameters in the shortwave part of the spectrum.

[20] Lognormal distribution functions were fitted to all impactor samples. As the wavelength dependent refractive index data of the MIM model [*D'Almeida et al.*, 1989] are given only for "water soluble", "mineral", "soot", and "water", we added all soluble ions (SO_4^{2-}, NO_3^-, Cl^-, NH_4^+, Na^+ and K^+) to create a synthetic impactor histogram of

water-soluble material and used this to obtain the lognormal function for the water soluble fraction. For the integration in the Mie calculations, 200 logarithmically evenly spaced size intervals were chosen (in the size range 0.03 to 10 μm). For each of these intervals, the masses of the components were calculated from the lognormal functions. The difference between the sum of the masses of all these species and of the total (gravimetric) mass was assigned to ''unidentified material'', which was assumed to have both the refractive index and the density of water. This ''unidentified material'' contains also all of the OC. Although we had measured OC data for all sites except Sonnblick, we did not use these data because of the lack of information on the wavelength dependent refractive index. For each interval, the mass concentrations of the species were converted to number concentrations using the geometric mean diameter of the size interval and the density of the components. The densities we used were 1000 kg/m^3 for both unidentified material and BC (a usual assumption for the density of BC), 2800 kg/m^3 for the minerals and 1530 kg/m^3 for the water soluble component, which corresponds e.g. to the apparent density found by *Pitz et al.* [2003]. The densities are also comparable to those used by other models (see the model intercomparison by *Kinne et al.* [2003] and the study by *Quinn et al.* [2001]).

[21] Part of the unidentified material certainly was water. Even if substrates are weighed at 50% humidity, which is the required humidity for PM measurements, water is still present in the aerosol deposits. In a recent study on the chemical mass closure of particulate matter, *Tsyro* [2005] reported that particle-bound water contributes on average 20–30% to the annual mean PM_{10} and $PM_{2.5}$ concentrations for the European aerosol. For two Austrian sites, Vienna and Streithofen (rural site, near Vienna), the calculated $PM_{2.5}$ water content was found to be 75–80% of the unidentified $PM_{2.5}$. In a similar study of PM_{10} and $PM_{2.5}$ in Switzerland, *Hueglin et al.* [2005] found that on average 10.6% of PM_{10} and 13–23% of $PM_{2.5}$ mass was water.

[22] Mie calculations were performed for assumed external and internal (homogeneous) volume mixtures of the components. Previous studies had shown that the Vienna aerosol is partially internally mixed with respect to both BC [*Hitzenberger and Tohno*, 2001] and TC [*Hitzenberger and Puxbaum*, 1993]. For the case of an internal mixture, we assumed a homogeneous volume mixture instead of particles consisting of a light-absorbing core with a nonabsorbing shell. The error introduced by this assumption is estimated at 20% at the most [*Seinfeld and Pandis*, 1998]. *Lesins et al.* [2002] found a difference of about 25% in forcing calculations for the assumptions of a homogeneous mixture and coated particles. *Jacobson* [2000] performed a study of the effect of mixing type of BC on radiative forcing. A core/shell type mixture gave a 50% higher forcing than a completely external mixture, and a 40% lower forcing than the homogeneous volume mixture. The assumptions on mixing type used in our study therefore give lower (external mixture) and higher (volume mixture) boundaries of forcing by BC containing aerosols.

[23] For the homogeneous volume mixture, the refractive index of the material in each small size interval was obtained by weighting the refractive index of each component with its mass fraction. Although the Maxwell-Garnett mixing rule should be used for internally mixed particles consisting of solid inclusions (BC) in a scattering medium (sulfates, etc.), we use the volume mixture because the study by *Lesins et al.* [2002] gave only small differences in forcing calculated with these two mixture rules. The mass-averaged density was also obtained in this way. For the external mixture assumption, the contribution of each component to the optical parameters was calculated separately.

[24] Water-soluble aerosol particles grow under conditions of elevated humidity. During humidity growth, the size, density and refractive index of the particles changes. We modeled the humidity growth by applying the mass growth factors measured earlier for the ambient aerosol in Vienna [*Hitzenberger et al.*, 1997] to the mass size distributions. These growth factors had been measured for 60, 70, 80 and 90% relative humidity (the ''dry'' sample mass had been determined at 50% humidity). In that study, the mass growth factors of the size segregated aerosol samples were rather independent of size in the fine size range (e.g., 2.4 at 90% humidity) and the coarse size range (1.4 at 90% humidity). Converted to growth factors in terms of particle diameter, they are in the range of factors used in other models [e.g., *Takemura et al.*, 2002; *Kinne et al.*, 2003].

[25] As the mass deposits on the impactor stages in our study had been weighed at humidities between 40 and 50%, the impactor-derived size distributions were taken as ''dry'' mass size distributions. In order to simulate the effect of elevated humidities on radiative forcing, we used the growth factors obtained by *Hitzenberger et al.* [1997] for the fine and coarse size ranges for particles of the fine and coarse modes, respectively, but only for calculations assuming an internally mixed aerosol. For a simulation of the humidity effect of an externally mixed aerosol, substance-specific growth factors would have been needed, which are not available.

3. Calculations of Radiative Forcing

[26] For purely scattering aerosols and cloud-free conditions, the box model proposed by *Charlson et al.* [1992] can be used to estimate the radiative effect. In our study, however, we estimated the regional direct forcing using the model proposed by *Haywood and Shine* [1995] for mixtures (internal or external) of absorbing and nonabsorbing species and cloud free conditions:

$$\Delta F(\lambda) = -F_0(\lambda)T_a^2(\lambda)\omega(\lambda)\beta\tau(\lambda) \cdot \left((1-R_s(\lambda))^2 - \frac{2R_s(\lambda)}{\beta}\left(\frac{1}{\omega(\lambda)}-1\right)\right) \quad (2)$$

where F_0 denotes the incident radiative flux at the top of the grid box, T_a the fractional transmittance of the atmosphere, ω the single-scattering albedo, β the fraction of radiation scattered upwards by the aerosol, τ the aerosol optical depth, R_s the surface albedo of the ground and λ the wavelength.

[27] For the calculation of the optical depth τ, the vertical distribution of the aerosol throughout the whole atmosphere should be known. As these data are unavailable, we used the concept of aerosol scale height. Modeling studies usually use scale heights of 2 km [e.g., *Schwartz*, 1996]. The recent studies by *Feczko et al.* [2002] and *Feczko et al.* [2005]

investigating the direct aerosol effect for nearby Hungary also use a scale height of 2 km (based on measurements by *Varhelyi* [1978]). We do not have data on aerosol scale height for our stations, but measurements of the annual variation of planetary boundary layer height (which contains most of the aerosol, but is lower than the scale height) in southern Germany [*Kreipl*, 2006] show average values between 1 (winter) and 3 km (summer). Under fair weather conditions in summer, the orographic convection systems carry boundary layer aerosols upslope, resulting in an alpine boundary layer height of 1–1.5 km above the mountain peaks [*Carnuth et al.*, 2002; *Carnuth and Trickl*, 2000; *Nyeki et al.*, 2002]. The sensitivity study, which is also included in the *Feczko et al.* [2005] paper, shows that radiative forcing is not strongly dependent on the assumed values of aerosol scale height (and errors in the value of the solar constant F_0). For this reason, we assumed a homogeneous aerosol distribution in a box with constant 2 km height even for the mountain stations and calculated the optical depth τ of this layer as a function of wavelength λ

$$\tau(\lambda) = \int_0^{\mathrm{H}} \sigma_{\mathrm{ext}}(\lambda)\mathrm{dz} = \sigma_{\mathrm{ext}}(\lambda)\mathrm{H} \tag{3}$$

with σ_{ext} the extinction coefficient obtained from the Mie calculations.

[28] For the incident solar flux at the top of the atmosphere, i.e., the incoming radiative flux we used $F_0 = 1/4\ S_0$. The values for the solar constant S_0 and the fractional transmittance T_a were set to 1368 W/m^2 and 0.79, respectively [e.g., *Lesins et al.*, 2002]. The wavelength dependence of the incoming solar radiation was assumed to follow Planck's equation for a black body with a temperature T = 6000 K. For the wavelength range above 4 μm, solar radiation provides hardly any input. The incident radiation in this wavelength range comes from the blackbody radiation of the surroundings, so the radiation emitted by a black body with a temperature of 288 K (the global annual average surface temperature) was assumed.

[29] The upscatter fraction β (fraction of light scattered into the upward hemisphere relative to the local horizon) depends on the particle size, wavelength and solar zenith angle [e.g., *Pilinis et al.*, 1995; *Nemesure et al.*, 1995]. Calculations of β are described by *Wiscombe and Grams* [1976] as an integral over the scattering phase function. *Charlson et al.* [1992] proposed an average value for β = 0.29 and *Haywood and Shine* [1995] suggested that the average value of β has to be reduced to 0.21, as a result of their Mie calculations for an aerosol number size distribution with mode radius 0.05 μm and standard deviation of 2, and for a wavelength of 700 nm. In the *IPCC* [2001] report, average values of $\beta = 0.22$ for polluted continental aerosols and $\beta = 0.21$ for background aerosols (with bimodal size distributions) are given. We used these values for the urban and mountain sites (regional background aerosol), respectively.

[30] A different surface albedo R_s was chosen for the sites. For the urban sites, R_s was assumed to be 0.16 (independent of wavelength). At the mountain sites, the ground was covered with snow or ice, so we chose $R_s = 0.35$ and 0.5 for the shortwave (below 4 μm) and longwave part of the spectrum for ice and R_s = 0.8 and 0.5 for the two wavelength ranges for fresh snow (all albedo values taken from *Roedel* [1994]). The influence of solar zenith angle on surface albedo was not taken into account.

[31] For each aerosol component, the scattering and absorption coefficients and single-scattering albedo are calculated for spherical particles at the 60 wavelengths and for dry conditions. For the internal mixture, calculations were also performed at four different relative humidities (60%, 70%, 80%, and 90%).

[32] Using all these input parameters, the model provides an estimate of the spectrally averaged radiative forcing ΔF (in W/m^2) due to scattering and absorption by the aerosol

$$\Delta \mathrm{F} = \Delta F_{\mathrm{SW}} + \Delta F_{\mathrm{LW}} = \frac{\sum_{\lambda \le 4\mu\mathrm{m}} \Delta F(\lambda) \cdot \Delta\lambda \cdot \mathrm{E}(\mathrm{T_S}, \lambda)}{\sigma T_S^4} + \frac{\sum_{\lambda) 4\mu\mathrm{m}} \Delta F(\lambda) \cdot \Delta\lambda \cdot \mathrm{E}(\mathrm{T_L}, \lambda)}{\sigma T_{\mathrm{L}}^4} \tag{4}$$

with σ the Stefan-Boltzmann constant and T the temperature (T_S = 6000 K for shortwave and T_L = 288 K for longwave forcing).

4. Results and Discussion

4.1. Chemical Composition

[33] As background information, Table 3 shows both the average chemical composition of the aerosol at all sites in percent of total mass and seasonal averages for Linz and Graz, where measurements were made both in winter (January) and summer (August). The contributions of the substances were calculated from the lognormal distributions fitted through the impactor data and not the impactor histograms themselves, because the lognormal functions were the basis for the calculation of the optical parameters. The large fractions of unidentified mass at all sites contain also organic carbon (OC). As no data on the wavelength-dependent refractive index were available, no estimation of OC was performed. TC and BC measurements at the sites, however, indicate that BC/TC fractions are of the order of 0.6 for the urban sites [e.g., *Puxbaum et al.*, 2004], and 0.478 at Rax (Hitzenberger, private communication, 2003), so the BC fractions can be used to estimate the contribution of OC to total aerosol mass at the sites if necessary. For the conversion of OC to particulate organic matter, *Puxbaum et al.* [2004] suggest a value of 1.3 for urban sites and 1.7 for background aerosols in Austria.

[34] BC contributions in Vienna (spring) are lower (approx. 4%) than in Linz (circa 6%) and Graz (around 10%). The percentage of BC at Graz and Linz varies only slightly with the season, although in winter a higher contribution of BC might be expected because of the necessity of space heating. The dual-site study in the area of Vienna by *Puxbaum et al.* [2004], however, showed that the contribution of space heating to BC is quite small (i.e., less than 30% maximum) nowadays because of the widespread use of "clean" fuels with low BC emissions (e.g., natural gas or district heating). Some seasonal difference was found for Graz and Linz in the percentage of unidentified mass, part of which might be explained by a higher

Table 3. Average Contribution of Chemical Analytes to Total Aerosol Mass Concentration in Percent[a]

Site	Ions	BC	Minerals	Unidentified
Vienna	35.9	3.9	11.0	49.0
Linz, all data	33.6	6.4	2.9	57.1
Linz, winter	38.9	6.4	3.1	51.7
Linz, summer	13.63	6.7	2.1	77.6
Graz, all data	35.3	10.4	1.9	52.5
Graz, winter	43.8	11.0	1.28	43.9
Graz, summer	18.2	9.4	3.3	69.2
Sonnblick	42.3	3.9	8.2	56.0
Rax	50.7	6.3	9.8	33.3

[a]Only those analytes used for the forcing calculations.

fraction of OC in the aerosol. The AUPHEP database (Puxbaum, private communication, 2004) gives monthly means of the OC fraction in total mass as 16% and 12% for August and January in Linz, while at Graz hardly any change in OC fraction was found (16.2 in August and 15.5% in January).

[35] The composition of the aerosol at the mountain sites is quite comparable to that at the urban sites. Similar findings exist from other background [e.g., *Puxbaum et al.*, 2004; *Hueglin et al.*, 2005] and mountain sites in central Europe. At the Jungfraujoch, e.g., the BC content of the aerosol in summer is comparable to values measured at lower elevations [e.g., *Lavanchy et al.*, 1999; *Krivacsy et al.*, 2001]. Earlier measurements at Sonnblick [*Kasper and Puxbaum*, 1998; *Seibert et al.*, 1998] showed that during summer (the time of our measurement campaign), Sonnblick also receives PBL air masses rather than air from the free troposphere. Measurements at Rax were performed under wintry conditions in March, but due to the relatively low elevation (1644 m) the site also received PBL air most of the time.

4.2. Direct Radiative Forcing, Dry Aerosol, Urban Sites

[36] For the comparison between the sites, median values were calculated for each measurement campaign. Table 4 shows these values for all sites and assumptions on mixing state for the dry aerosol. In the urban aerosol and under the assumption of internal mixing, the largest negative forcing was found for the Linz campaign (total forcing -3.56 W/m^2), followed by Vienna (-2.16 W/m^2) and Graz (-0.77 W/m^2).

[37] As an example of the variability, Figure 1 gives the forcing for each day of the Vienna campaign both for the internally and externally mixed aerosol. For the externally mixed aerosol, forcings are even more negative (Linz: -5.83 W/m^2, Vienna -3.07 W/m^2 and Graz -4.46 W/m^2). All these forcings are much larger than the global average given by the IPCC report for sulfate aerosols alone (-0.44 W/m^2). As total forcing depends linearly on the total aerosol concentration, this difference could be explained by the much higher aerosol load at the urban sites compared to global average concentrations.

[38] Although no similar calculations (using measured size distributions and chemical composition of the aerosol) are available for European aerosols, some data on radiative forcing based on aerosol measurements in Europe exist. *Feczko et al.* [2002] calculated shortwave forcing by sulfate at a Hungarian background site as -2.4 W/m^2 and shortwave forcing by carbonaceous aerosols as -1 W/m^2 in summer. For fall aerosol at the same site, *Feczko et al.* [2005] give similar values for sulfate, but a positive value of $+0.4$ W/m^2 for shortwave forcing by carbonaceous particles.

[39] Estimations for aerosol forcing in Europe are available from global models (e.g., *Takemura et al.* [2002] give values of -5 W/m^2 to -10 W/m^2 for summer aerosols in Europe, North America and East Asia). For urban aerosols, some data are available for Asia. Based on aerosol measurements in Bangalore, India, *Babu et al.* [2002] calculated a top of the atmosphere forcing of $+5$ W/m^2 for an aerosol with a large fraction of BC in submicron mass (23%). A similar study in Pune, India found top of the atmosphere shortwave forcings between -7 W/m^2 and $+9$ W/m^2. A study conducted on Mt. Gibbes in North Carolina, USA [*Im et al.*, 2001], gave a 15% reduction of the aerosol cooling effect caused by light absorption by BC in the aerosol (forcing values from this study are given per unit optical depth and are consequently not comparable to our data here).

Table 4. Total Forcing, All Sites, for the Assumption of Internally and Externally Mixed Aerosols[a]

Site	Forcing Wm^{-2}, Dry Aerosol		Surface Albedo	Forcing Wm^{-2}, 90% Humidity, Internal mixture
	Internal Mixture	External Mixture		
Vienna	−2.16	−3.07	0.16	−5.18
Linz, all data	−3.56	−5.83	0.16	−13.42
Linz, winter	−3.80	−6.24	0.16	−13.42
Linz, summer	−2.53	−3.78	0.16	n.d.
Graz, all data	−0.77	−4.46	0.16	−9.12
Graz, winter	−1.11	−6.93	0.16	−13.98
Graz, summer	0.20	−1.29	0.16	−2.89
Sonnblick	1.61	0.01	0.35	0.16
	4.82	1.5	0.5	5.82
	9.86	4.18	0.8	11.63
Rax	0.95	0.3	0.35	0.6
	1.95	1.1	0.5	1.99
	3.87	2.53	0.8	4.52

[a]The last column gives the forcing calculated for a relative humidity of 90%. All other values were calculated for the dry aerosol. For Linz, summer, no median value was calculated for 90% humidity, as only few valid data points were available (the other data points were rejected because of problems in calculating the optical parameters). All of the data for the direct radiative forcing are based on the assumption that at every site the boundary layer height above that site is equal to 2 km.

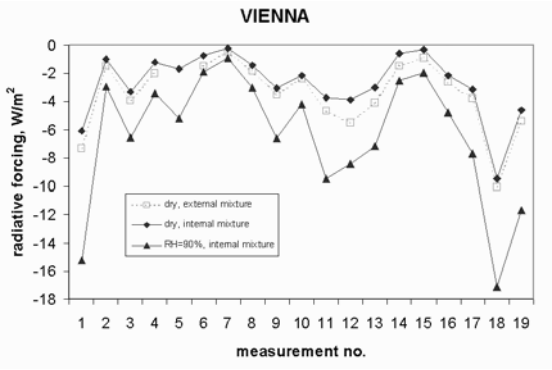

Figure 1. Total forcing by the Vienna aerosol during the whole campaign. The full symbols denote the forcing calculated assuming an internal mixture, while the open symbols show the results obtained with the assumption of an external mixture.

[40] The less negative forcing in the case of internally mixed aerosols is expected, because BC gives a larger specific absorption coefficient [*Ackerman and Toon*, 1981; *Martins et al.*, 1998; *Jacobson*, 2000] and consequently a lower single-scattering albedo when it is mixed internally to the aerosol, creating a positive contribution to total forcing. The relatively low negative forcing calculated for the internally mixed Graz aerosol can be explained by the large contribution of BC to the total aerosol (10.43% of total mass) and the low mass median diameter of BC (average: 0.43 μm). The Vienna and Linz aerosols contained less BC (3.91 and 6.43%, respectively) with larger mass median diameters (0.48 and 0.46 μm, respectively). Single-scattering albedo at 0.55 μm, a wavelength usually considered representative for the total spectrum [*Lesins et al.*, 2002] was consequently lowest in Graz (0.74 and 0.86 for the internally and externally mixed aerosol), followed by Linz (0.834 and 0.92) and Vienna (0.889 and 0.931).

[41] Seasonal differences in forcing can be investigated for the Graz and Linz data. At both sites, a campaign was conducted in January and one in August of 2001. Table 4 also shows the forcings obtained for the sites as seasonal medians. Forcings in wintertime are more negative than in summer at both sites, and forcings calculated for the external mixture more negative than for internally mixed aerosols. Surface albedo (see below) had no influence on these calculations, as a fixed value of 0.16 was used at the urban sites for all seasons.

[42] In the case of an externally mixed aerosol, calculations of the contributions of the component classes are possible. Figures 2a, 2b, and 2c show the results for the urban sites (dry aerosol). As expected, BC gives positive forcings in all cases with a minimum value in Vienna (+0.34 W/m^2) followed by Linz (+1.18 W/m^2) and Graz (+2.14 W/m^2), an order which corresponds to the BC content of the aerosols at these sites (Table 3). Except for Vienna, these forcings are larger than the literature values (+0.2 W/m^2, *IPCC* [2001]; +0.5 W/m^2, *Sato et al.* [2003]; +0.51 W/m^2, *Chung and Seinfeld* [2002]). In the region of our study, BC seems to contribute more to total aerosol forcing than the usual global average values. Simulations of the annual direct radiative forcing of BC reported by *Takemura et al.* [2002] for the Northern Hemisphere yield a value of +0.32 W/m^2, which is in good agreement with our results. An extensive comparison of the total direct aerosol forcing calculated at AERONET (Aerosol Robotic Network) sites and simulated with seven 3-D models on a seasonal basis [*Kinne et al.*, 2003] shows direct radiative forcing at the AERONET sites is usually larger than global forcing averages because of the proximity of these sites to aerosol sources, where many models underestimate the aerosol source strength. As an example, direct radiative forcing values estimated from AERONET measurements at Ispra (Italy) range from -3 to -8 W/m^2 at the top of the atmosphere, which is of the same order of magnitude as the values calculated in the present study. *Liepert and Tegen*

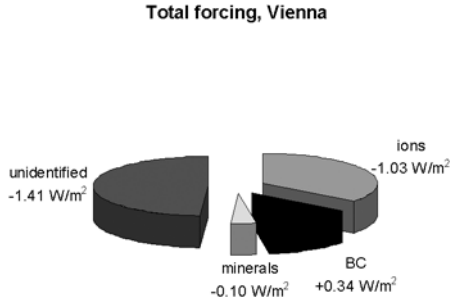

Figure 2a. Contribution of component classes to total forcing at urban sites (Vienna, Linz, Graz); external mixture, dry aerosol.

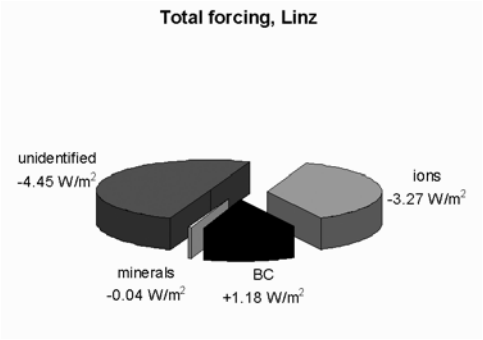

Figure 2b. As in Figure 2a.

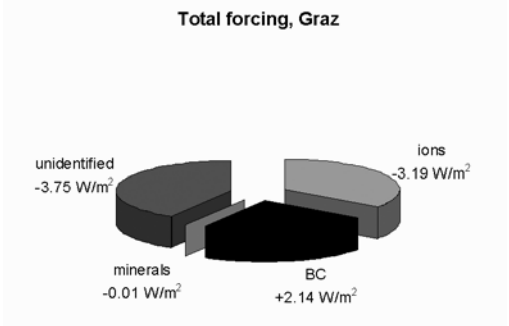

Figure 2c. As in Figure 2a.

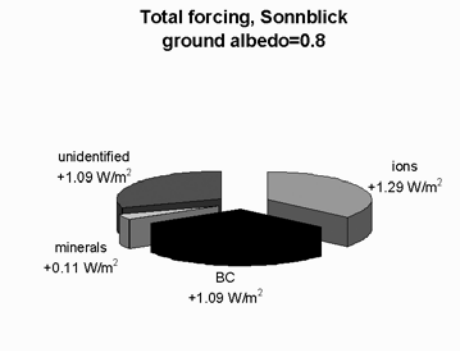

Figure 3a. Contribution of components to total forcing at the mountain sites (Sonnblick, Rax). Assumptions: dry aerosol, external mixture, ground albedo 0.8 (corresponding to fresh snow).

[2002] also use AERONET data and find the variability of optical properties within a grid point quite large.

[43] At all sites, the large fraction of unidentified mass, which is assigned the optical properties of water in our model, dominated the forcing estimates. The mineral components gave only a small forcing, which is in keeping with their low contributions to total mass.

[44] The study of *Takemura et al.* [2002] on the global distribution of single-scattering albedo and radiative forcing of various aerosol species using an aerosol transport model coupled with an atmospheric general circulation model gave values of single-scattering albedo for our region of interest slightly over 0.9 and direct forcing values between -5 and -10 W/m^2 at the top of the atmosphere. In this study, however, values of surface albedo are much lower (0.07) than the ones we used.

4.3. Direct Radiative Forcing, Dry Aerosol, Mountain Sites

[45] At the mountain sites, different values of ground albedo were used to account for the effects of ice or snow as a ground cover. At Sonnblick, measurements were performed in summertime, so the albedo of ice is appropriate for this station, which is at the edge of a glacier. At Rax an even higher surface albedo should be applicable because the ground was covered with fresh snow all during the campaign. Table 4 shows also the effect of ground albedo on total forcing for both internal and external mixtures at the background sites (dry aerosol).

[46] At the mountain sites, all forcings are positive. The internal mixing assumption again gives more positive forcings than the assumption of external mixing. With increasing ground albedo, forcings become even more positive, which means that the warming effect of the aerosol increases. The extreme value is obtained at Sonnblick (internal mixture: +9.86 W/m^2 for ground covered by snow, and +1.61 W/m^2 for ground covered by ice).

[47] Such an extremely large positive forcing could be caused by very high BC fractions in the aerosol. In our study, BC fractions in the background aerosol are comparable to those found at the urban sites (Rax: 6.3%, Sonnblick: 3.9%), so the large positive forcing is caused not only by BC itself but by the combination of an absorbing aerosol above a highly reflective surface. Single-scattering albedos at the sites were 0.841 and 0.918 (internal and external mixture) at Rax and 0.88 and 0.94 at Sonnblick. In a study of the radiative effect of a certain amount of BC in Arctic aerosols, *Coakley et al.* [1983] showed that aerosol radiative forcing can turn from negative to positive for a fixed single-scattering albedo when ground albedo is increased. The same effect is reported in the study by *Roberts and Jones* [2004], who found a larger positive effect of BC over the deserts (high surface albedo) surrounding the Mediterranean Sea than over the sea itself (low surface albedo).

[48] Extrapolating these findings to wintertime urban aerosol, the same effect can be seen in our data: the negative forcings we found in the shortwave range for the urban sites could turn to positive in wintertime when the ground is covered with fresh snow, or when the ground reflects more light than the dark urban roof or asphalt surfaces.

[49] As an extreme case, the contribution of the components to total forcing is shown in Figures 3a and 3b for the case of an externally mixed dry aerosol and a very high ground albedo of 0.8 (fresh snow). At both mountain sites, forcing is dominated by BC, and even the forcing by the ions is positive. Above the highly reflecting ground cover, the weak absorption of the ions in the longwave part of the spectrum becomes noticeable. Even though the unidentified mass is not so different at the mountain sites compared to the urban sites (Table 3), its contribution to total forcing is rather small because of the large effect caused by an absorbing aerosol (BC) above a highly reflective ground.

[50] The positive forcing of the aerosol at the mountain sites might be interesting not merely for the direct effect on climate, but also for the semidirect effect. The mountain sites are at heights where clouds are formed. The Rax site, e.g., is within cloud circa 50% of the time. At Sonnblick, in-cloud conditions prevail circa 70% of the time (ZAMG, personal communication, 2002). Under these circumstances the effect of positive aerosol forcing on the ambient temperature might already play a role in cloud formation and/or evaporation.

4.4. Influence of Relative Humidity

[51] Figure 4 shows the influence of relative humidity on the forcings calculated for the aerosol at the urban (Figure 4a) and mountain sites (Figure 4b). Campaign median values at 90% humidity are given also in Table 4. These calculations were performed only for the case of an

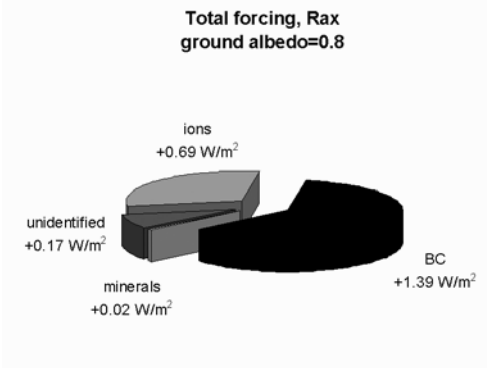

Figure 3b. As in Figure 3a.

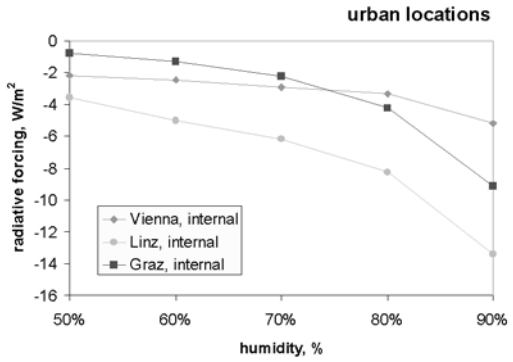

Figure 4a. Dependence of calculated total forcings on relative humidity (assumption: internal mixture) for the urban locations (Vienna: diamonds, Graz: squares, Linz: circles).

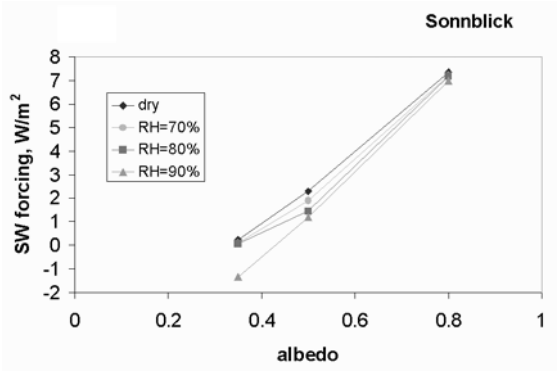

Figure 5a. Influence of ground albedo and relative humidity on shortwave forcing (internally mixed aerosol): (a) Sonnblick; (b) Rax.

internally mixed aerosol, as the mass growth factors we used had been measured [*Hitzenberger et al.*, 1997] on deposited aerosol samples, which are necessarily internally mixed. Identical growth factors were used for the aerosol at all sites.

[52] The effect of humidity is different for the two types of sites. At the urban sites, forcings become more negative with increasing humidity. The forcing for the Vienna aerosol, e. g. changes from -2.16 W/m^2 to -5.18 W/m^2 when humidity changes from 50% to 90%. The factor of change for Graz is about 3 times larger than that for Linz (3.8), and about 5 times greater than that for Vienna (2.4). At the mountain stations, a very small change is found in the case of the high ground albedo (0.8, snow); the factor of change is smaller than at the urban sites (about 1.2 for both Rax and Sonnblick sites). In the case of the lower ground albedo (0.35, ice), hardly any change is found in forcing values with increasing humidity; the factor of change is 0.6 for Rax, and 0.1 for Sonnblick). Absorption by BC dominates the forcing to such an extent that the change in particle size and refractive index due to the uptake of water does not affect the forcing.

[53] In Austria, humidities usually are intermediate to high. Daily minimum values of humidity are measured at 14:00 Central European Time (i.e., UTC + 1 hour), while mornings and afternoons are usually more humid. Long-term monthly average humidities in Vienna at 14:00 range between 50% in May and 75% in December. For Graz, the 14:00 average humidities are rather similar with 49% in April and 84% in December (ZAMG, personal communication, 2002). For the urban sites, the forcings given in Table 4 for the dry aerosol are therefore lower boundaries under no-snow conditions. For spring and summer, radiative forcing by the urban aerosol will be quite well represented by the ''dry'' values in Table 4 or maybe the values for 60 or 70% in Figures 4a and 4b, while in wintertime the values for 90% humidity will be more appropriate under no-snow conditions.

4.5. Combined Influence of Humidity and Ground Albedo for the Mountain Sites

[54] The combined effect of ground albedo and relative humidity is investigated further the for shortwave forcing (spectral range 0.3–4.0 μm) in the case of mountain sites (Figure 5a for Sonnblick, Figure 5b for Rax), where shortwave forcing values obtained from calculations with an intermediate ground albedo of 0.5 are also shown. A humidity effect is seen only for the low ground albedo of

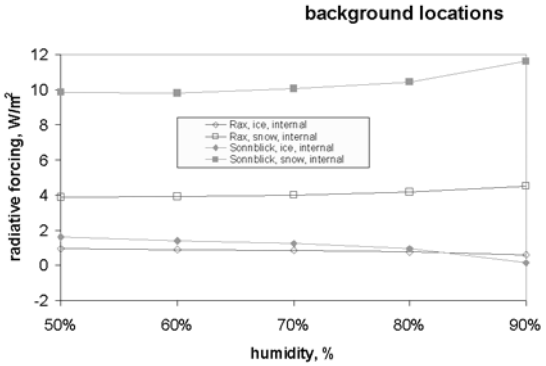

Figure 4b. Dependence of calculated total forcings on relative humidity (assumption: internal mixture) for the mountain sites (Sonnblick: full symbols, Rax: open symbols) for ground albedo values representative of ice (diamonds) and fresh snow (squares).

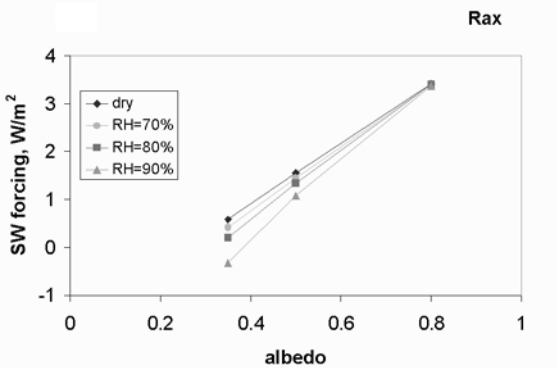

Figure 5b. As in Figure 5a.

0.35, where forcings change from positive to negative at both sites when humidity increases from 50% (dry aerosol) to 90%. With increasing ground albedo, the humidity effect becomes smaller and shortwave forcings are positive for all humidities.

[55] If these findings are extrapolated to the urban sites with snow cover on the ground or to more arid sites, humidity effects on total forcing will be smaller than without snow or dry ground. A general conclusion about the humidity effect on radiative forcing at a certain site cannot be drawn without considering the effect of surface albedo.

5. Summary and Conclusions

[56] The results of our study show that the central European aerosols have a much larger (negative) forcing than the global average values such as the -0.44 W/m^2 given by the IPCC report [*IPCC*, 2001] for sulfate aerosols. For the urban areas, forcings were between -3.56 W/m^2 (Linz) and -0.77 W$\neq$m^2 (Graz) under the assumption of internal mixing and dry aerosol (50% humidity). The assumption of external mixing led to even larger negative forcings ranging from -5.83 W/m^2 (Linz) to -3.07 W/m^2 (Vienna). At the mountain sites, BC plays a much more important role because of the high ground albedo of ice (shortwave albedo: 0.35, longwave: 0.5) and snow (0.8 and 0.5, respectively) compared to the urban surface albedo of 0.16. All calculated forcings for the mountain stations are positive ranging up to +9.86 W/m^2 (Sonnblick, internally mixed aerosol, dry conditions), although the BC content of the urban aerosols was larger both in Linz (6.4%) and Graz (10.4%) than at Sonnblick and Vienna (3.9%). Under conditions of elevated relative humidity, forcings for the urban sites become more negative. For Vienna, e. g., the forcing calculated for internally mixed aerosol changes from -2.16 W/m^2 at 50% humidity to -5.18 W/m^2 at 90% humidity. If the aerosols are assumed to be internally mixed rather than externally, negative forcings are smaller because of the enhanced absorption by internally mixed BC. Even though the chemical composition of urban and mountain aerosols is rather similar, calculated forcings at the mountain sites are much less negative or even positive because of the higher surface albedo (snow or ice compared to dark urban surfaces). If these findings are extrapolated to urban areas in wintertime with high humidities and snow-covered ground, the data presented here give an overview of the range of forcings to expect under typical meteorological and seasonal conditions in central Europe. The data presented in this study also give an overview of the variation of radiative forcing in a relatively small area, which is about the size of a grid point of a typical global aerosol model.

[57] **Acknowledgments.** The financial support by Austrian Science Fund FWF (Vienna and Rax data P 13143-CHE, Sonnblick data P 10328-CHE) is gratefully acknowledged. The Linz and Graz data were collected during the project AUPHEP, funded by the Ministry for the Environment, Youth and Family Affairs and the Ministry for Science and Traffic (contract 144440/45-I/4/98), and the Austrian Academy of Sciences. Additional contributions have been made by the ambient air monitoring networks of the Austrian Provinces, the Federal Environmental Agency, and several companies. G. Iorga was recipient of a Marie Curie fellowship (contract HPMT-CT-2001-00400). We thank the Zentralanstalt für Meteorologie und Geodynamik (ZAMG), Vienna, for the information on long-term averages of monthly humidities.

References

Ackerman, A. S., O. S. Toon, D. E. Stevens, A. J. Heymsfield, V. Ramanathan, and E. J. Welton (2000), Reduction of tropical cloudiness by soot, *Science*, *288*, 1042–1047.

Ackerman, T. P., and O. B. Toon (1981), Absorption of visible radiation in atmospheres containing mixtures of absorbing and non-absorbing particles, *Appl. Opt.*, *20*, 3661–3668.

Albrecht, B. A. (1989), Aerosols, cloud microphysics, and fractional cloudiness, *Science*, *245*, 1227–1230.

Babu, S. S., S. K. Satheesh, and K. K. Moorthy (2002), Aerosol radiative forcing due to enhanced black carbon at an urban site in India, *Geophys. Res. Lett.*, *29*(18), 1880, doi:10.1029/2002GL015826.

Bates, T. S., P. K. Quinn, D. J. Coffman, J. E. Johnson, and A. M. Middlebrook (2005), Dominance of organic compounds in the marine boundary layer over the Gulf of Maine during NEAQS 2002 and their role in aerosol light scattering, *J. Geophys. Res.*, *110*, D18202, doi:10.1029/2005JD005797.

Bohren, C., and D. R. Huffman (1983), *Absorption and Scattering of Light by Small Particles*, John Wiley, Hoboken, N. J.

Bond, T. C., D. G. Streets, K. F. Yarber, S. M. Nelson, J.-H. Woo, and Z. Klimont (2004), A technology-based global inventory of black and organic carbon emissions from combustion, *J. Geophys. Res.*, *109*, D14203, doi:10.1029/2003JD003697.

Cachier, H., M. P. Bremond, and P. Buat-Ménard (1989), Determination of atmospheric soot carbon with a simple thermal method, *Tellus, Ser. B*, *41*, 379–390.

Carnuth, W., and T. Trickl (2000), Transport studies with the IFU three-wavelength aerosol lidar during the VOTALP Mesolcina experiment, *Atmos. Environ.*, *34*, 1425–1434.

Carnuth, W., U. Kempfer, and T. Trickl (2002), Highlights of the tropospheric Lidar studies at IFU within the TOR project, *Tellus, Ser. B*, *54*, 163–185.

Charlson, R. J., S. E. Schwartz, J. M. Hales, R. D. Cess, J. A. Coakley, J. E. Hansen, and D. J. Hofmann (1992), Climate forcing by anthropogenic aerosols, *Science*, *255*, 423–430.

Chung, S. H., and J. H. Seinfeld (2002), Global distribution of climate forcing of carbonaceous aerosols, *J. Geophys. Res.*, *107*(D19), 4407, doi: 10.1029/2001JD001397.

Coakley, J. A., R. D. Cess, and F. B. Yurevich (1983), The effect of tropospheric aerosols on the Earth's radiation budget: A parameterization for climate models, *J. Atmos. Sci.*, *40*, 116–138.

Cooke, W. F., and J. J. N. Wilson (1996), A global black carbon aerosol model, *J. Geophys. Res.*, *101*(D14), 19,395–19,409.

D'Almeida, G. A., P. Koepke, and M. Hess (1989), The Meteorological Institute Munich (MIM) optical aerosol Climatology, *BMFT Forschungsber. KF-1011*, 271 pp., Bundesminist. für Forsch. und Technol., Munich, Germany.

Feczko, T., A. Molnar, E. Meszaros, and G. Major (2002), Regional climate forcing of aerosol estimated by a box model for a rural site in central Europe during summer, *Atmos. Environ.*, *36*, 4125–4131.

Feczko, T., A. Marton, A. Molnar, and G. Szentes (2005), Estimation of direct radiative forcing of the aerosol for a rural site in central Europe, *Atmos. Environ.*, *39*, 7127–7136.

Hansen, J. E., M. Sato, and R. Ruedy (1997), Radiative forcing and climate response, *J. Geophys. Res.*, *102*(D6), 6831–6864.

Hauck, H., A. Berner, T. Frischer, B. Gomiscek, M. Kundi, M. Neuberger, H. Puxbaum, and O. Preining (2004), AUPHEP: Austrian Project on Health Effects of Particulates—General overview, *Atmos. Environ.*, *38*, 3905–3918.

Haywood, J. M., and K. P. Shine (1995), The effect of anthropogenic sulfate and soot aerosol on the clear sky planetary radiation budget, *Geophys. Res. Lett.*, *22*(5), 603–606.

Heintzenberg, J. (1982), Size-segregated measurements of particulate elemental carbon and aerosol light absorption at remote Arctic locations, *Atmos. Environ.*, *16*, 2461–2469.

Hess, M., P. Koepke, and I. Schult (1998), Optical properties of aerosols and clouds: The software package OPAC, *Bull. Am. Meteorol. Soc.*, *79*, 831–844.

Hitzenberger, R., and H. Puxbaum (1993), Comparisons of the measured and calculated specific absorption coefficient for Vienna urban aerosol samples, *Aerosol Sci. Technol.*, *18*, 323–336.

Hitzenberger, R., A. Berner, U. Dusek, and R. Alabashi (1997), Humidity-dependent growth of size-segregated aerosol samples, *Aerosol Sci. Technol.*, *27*, 116–130.

Hitzenberger, R., A. Berner, R. Kromp, A. Kasper-Giebl, A. Limbeck, W. Tscherwenka, and H. Puxbaum (2000), Black carbon and ionic species at a high-elevation European site (Mt. Sonnblick, 3106 m, Austria):

Concentrations and scavenging efficiencies, *J. Geophys. Res.*, *105*(D20), 24,637–24,646.
Hitzenberger, R., and S. Tohno (2001), Comparison of black carbon (BC) aerosols in two urban areas (Uji, Japan and Vienna, Austria): Concentrations and size distributions, *Atmos. Environ.*, *35*, 2089–2100.
Hitzenberger, R., A. Berner, H. Giebl, K. Drobesch, A. Kasper-Giebl, M. Loeflund, H. Urban, and H. Puxbaum (2001), Black carbon (BC) in Alpine aerosols and cloud water concentrations and scavenging efficiencies, *Atmos. Environ.*, *35*, 5135–5141.
Hitzenberger, R., J. Tursic, I. Grgic, A. Berner, P. Ctyroky, and B. Podkrajsek (2006), Particle size distribution of carbon in aerosols collected in Vienna and Ljubljana, *Chemosphere*, *65*, 2106–2113.
Hueglin, A., R. Gehrig, U. Baltensperger, M. Gysel, C. Monn, and H. Vonmont (2005), Chemical characteristics of PM2.5, PM10 and coarse particles at urban, near-city and rural sites in Switzerland, *Atmos. Environ.*, *39*, 637–651.
Im, J.-S., V. K. Saxena, and B. N. Wenny (2001), Temporal trends of black carbon concentration and regional climate forcing in the southeastern United States, *Atmos. Environ.*, *35*, 3293–3302.
IPCC (2001), *Climate Change 2001: The Scientific Basis. Contribution of Working Group I to the Third Assessment Report of the Intergovernmental Panel on Climate Change*, edited by J. T. Houghton et al., 881 pp., Cambridge Univ. Press, New York.
Jacobson, M. Z. (2000), A physically-based treatment of elemental carbon optics: Implications for global direct forcing of aerosols, *Geophys. Res. Lett.*, *27*, 217–220.
Kasper, A., and H. Puxbaum (1998), Seasonal variation of SO_2, HNO_3, NH_3 and selected aerosol components at Sonnblick (3106 m asl), *Atmos. Environ.*, *32*, 3925–3939.
Kinne, S., et al. (2003), Monthly averages of aerosol properties: A global comparison among models, satellite data, and AERONET ground data, *J. Geophys. Res.*, *108*(D20), 4634, doi:10.1029/2001JD001253.
Kreipl, S. (2006), Messung des Aeorsoltransports am Alpennordrand mittels Laserradar (Lidar), Ph.D. thesis, Friedrich-Alexander-Universtität Erlangen-Nürnberg, Erlangen, Germany.
Krivacsy, Z., A. Hoffer, Z. Sarvari, D. Temesi, U. Baltensperger, S. Nyeki, E. Weingartner, S. Kleefeld, and S. G. Jennings (2001), Role of organic and black carbon in the chemical composition of atmospheric aerosol at European background sites, *Atmos. Environ.*, *35*, 6231–6244.
Lavanchy, V. M. H., H. W. Gaggeler, S. Nyeki, and U. Baltensperger (1999), Elemental carbon (EC) and black carbon (BC) measurements with a thermal method and an aethalometer at the high-alpine research station Jungfraujoch, *Atmos. Environ.*, *33*(17), 2759–2769.
Lesins, G., P. Chylek, and U. Lohmann (2002), A study of internal and external mixing scenarios and its effect on aerosol optical properties and direct radiative forcing, *J. Geophys. Res.*, *107*(D10), 4094, doi:10.1029/2001JD000973.
Liepert, B., and I. Tegen (2002), Multidecadal solar radiation trends in the United States and Germany and direct tropospheric aerosol forcing, *J. Geophys. Res.*, *107*(D12), 4153, doi:10.1029/2001JD000760.
Lürzer, C. (1980), Über die Bestimmung von multimodalen Größenverteilungen atmosphärischer Aerosole mittels Unterdruck-Kaskadenimpaktoren, Ph.D. thesis, University of Vienna, Austria.
Martins, J. V., P. Artaxo, C. Liousse, J. S. Reid, P. V. Hobbs, and Y. J. Kaufman (1998), Effects of black carbon content, particle size, and mixing on light absorption by aerosols from biomass burning in Brazil, *J. Geophys. Res.*, *103*(D24), 32,041–32,050.
Nemesure, S., R. Wagener, and S. E. Schwartz (1995), Direct shortwave forcing of climate by the anthropogenic sulfate aerosol: Sensitivity to particle size, composition and relative humidity, *J. Geophys. Res.*, *100*(D12), 26,105–26,116.
Nyeki, S., K. Eleftheriadis, U. Baltensperger, I. Colbeck, M. Fiebig, A. Fix, C. Kiemle, M. Lazaridis, and A. Petzold (2002), Airborne Lidar and in-situ aerosol observations of an elevated layer, leeward of the European Alps and Apennines, *Geophys. Res. Lett.*, *29*(17), 1852, doi:10.1029/2002GL014897.
Novakov, T., M. O. Andreae, R. Gabriel, T. W. Kirchstetter, O. L. Mayol-Bracero, and V. Ramanathan (2000), Origin of carbonaceous aerosols over the tropical Indian Ocean: Biomass burning or fossil fuels?, *Geophys. Res. Lett.*, *27*, 4061–4064.
Penner, J. E., C. C. Chuang, and K. Grant (1998), Climate forcing by carbonaceous and sulfate aerosols, *Clim. Dyn.*, *14*, 839–851.
Pilinis, C., S. N. Pandis, and J. H. Seinfeld (1995), Sensitivity of direct climate forcing by atmospheric aerosols to aerosol size and composition, *J. Geophys. Res.*, *100*(D9), 18,739–18,754.
Pincus, R., and M. A. Baker (1994), Effect of precipitation on the albedo susceptibility of clouds in the marine boundary layer, *Nature*, *372*, 250–252.
Pitz, M., J. Cyrys, E. Karg, A. Wiedensohler, H. E. Wichmann, and J. Heinrich (2003), Variability of apparent particle density of an urban aerosol, *Environ. Sci. Technol.*, *37*, 4336–4342.
Putaud, J.-P., et al. (2004), A European aerosol phenomenology: 2. Chemical characteristics of particulate matter at kerbside, urban, rural and background sites in Europe, *Atmos. Environ.*, *38*, 2579–2595.
Puxbaum, H., and J. Rendl (1983), An automated system for the detection of carbon and sulfur in airborne particles, *Mikrochim. Acta*, *1*(3–4), 263–272.
Puxbaum, H., B. Gomiscek, M. Kalina, H. Bauer, A. Salam, S. Stopper, O. Preining, and H. Hauck (2004), A dual site study of PM2.5 and PM10 aerosol chemistry in the larger region of Vienna, Austria, *Atmos. Environ.*, *38*, 3949–3958.
Quinn, P. K., D. J. Coffman, T. S. Bates, T. L. Miller, J. E. Johnson, K. Voss, E. J. Welton, and C. Neususs (2001), Dominant aerosol chemical components and their contribution to extinction during the Aerosols99 cruise across the Atlantic, *J. Geophys. Res.*, *110*(D18), 20,783–20,809.
Quinn, P. K., D. J. Coffman, T. S. Bates, T. L. Miller, J. E. Johnson, E. J. Welton, C. Neususs, M. Miller, and P. J. Sheridan (2002), Aerosol optical properties during INDOEX 1999: Means, variability, and controlling factors, *J. Geophys. Res.*, *107*(D19), 8020, doi:10.1029/2000JD000037.
Roberts, D., and A. Jones (2004), Climate sensitivity to black carbon aerosol from fossil fuel combustion, *J. Geophys. Res.*, *109*, D16202, doi:10.1029/2004JD004676.
Roedel, W. (1994), *Physik unserer Umwelt. Die Atmosphäre*, Springer, Berlin.
Sato, M., J. E. Hansen, D. Koch, A. Lacis, R. Ruedy, O. Dubovik, B. Holben, M. Chin, and T. Novakov (2003), Global atmospheric black carbon inferred from AERONET, *Proc. Natl. Acad. Sci.*, *100*, 6319–6324.
Schaap, M., H. A. C. D. Van Der Gon, F. J. Dentener, A. J. H. Visschedijk, M. Van Loon, H. M. ten Brink, J.-P. Putaud, B. Guillaume, C. Liousse, and P. J. H. Builtjes (2004), Anthropogenic black carbon and fine aerosol distribution over Europe, *J. Geophys. Res.*, *109*, D18207, doi:10.1029/2003JD004330.
Schwartz, S. E. (1996), The whitehouse effect: Shortwave radiative forcing of climate by anthropogenic aerosols: an overview, *J. Aerosol Sci.*, *27*, 359–382.
Seibert, P., H. Kromp-Kolb, A. Kasper, M. Kalina, H. Puxbaum, D. T. Jost, M. Schwikowski, and U. Baltensperger (1998), Transport of polluted boundary layer air from the Po Valley to high-alpine sites, *Atmos. Environ.*, *23*, 3953–3965.
Seinfeld, J. H., and S. N. Pandis (1998), *Atmospheric Chemistry and Physics. From Air Pollution to Climate Change*, 1326 pp., Wiley-Interscience, Hoboken, N. J.
Takemura, T., T. Nakajima, O. Dubovik, B. N. Holben, and S. Kinne (2002), Single scattering albedo and radiative forcing of various aerosol species with a global three-dimensional model, *J. Clim.*, *15*(4), 333–352.
Tsyro, S. G. (2005), To what extent can aerosol water explain the discrepancy between model calculated and gravimetric PM_{10} and $PM_{2.5}$?, *Atmos. Chem. Phys.*, *5*, 515–532.
Twomey, S. (1977), The influence of pollution on the shortwave albedo of clouds, *J. Atmos. Sci.*, *34*, 1149–1152.
Varhelyi, G. (1978), On the vertical distribution of sulphur compounds in the lower troposphere, *Tellus*, *30*, 542–545.
Wiscombe, W. J., and G. W. Grams (1976), The backscattered fraction in two-stream approximations, *J. Atmos. Sci.*, *33*, 2440–2451.

R. Hitzenberger, Institute for Experimental Physics, University of Vienna, Boltzmanngasse 5, A-1090 Vienna, Austria. (regina.hitzenberger@univie.ac.at)

G. Iorga, Department of Physics, Faculty of Chemistry, University of Bucharest, Regina Elisabeta Avenue, No. 4–12, 030018 Bucharest, Romania.

A. Kasper-Giebl and H. Puxbaum, Institute for Chemical Technology and Analytics, Vienna University of Technology, Getreidemarkt 9, A1060 Vienna, Austria.